ce/papers Proceedings in civil engineering

Ernst & Sohn A Wiley Brand

Check for updates

ORIGINAL ARTICLE

eurosteel AMSTERDAM 2023

Ernst & Sohn A Wiley Brand

Experimental and numerical investigation of reduced web section connections in fire

Yabari Oday[1], Alanen Mika[2], Malaska Mikko[2], Cashell Katherine A.[1]

Correspondence

Dr K.A. Cashell
University College London
Gower Street
London, UK
Email: k.cashell@ucl.ac.uk

[1] UCL, UK
[2] Tampere University, Finland

Abstract

This paper presents the details and analysis of a fire test conducted on a reduced web section (RWS) connection for steel framed construction. The test was completed in the fire laboratory at Tampere University in order to assess how these connections, usually selected and designed for their seismic performance, behave under fire conditions. RWS connections were first devised for fixed joints in steel framed buildings, with a view to moving the plastic hinge away from the column face during an extreme event such as an earthquake, thus improving the ductility of the structure. Until now, there was very little known of their behaviour under fire conditions. Accordingly, the current paper provides a detailed description and analysis of the fire test on a RWS connection, during which the arrangement lasted for around 16 minutes of standard fire exposure. It also describes the development of a numerical model, which is validated against the test data. The purpose of the model is to enable a more thorough examination of the various parameters and variables that may exist in a real structure, subjected to a real fire.

Keywords

Steel structures; finite element modelling; joints; fire test; RWS connection

1 Introduction

This paper is concerned with the behaviour of steel moment frames with reduced web section (RWS) connections under fire conditions. The reduced web section is achieved by introducing openings in the web of the steel beams, adjacent to the joint, similar to those which exist in cellular beams. RWS connections were initially devised in the 1990's for use in steel framed buildings in regions susceptible to seismic events, after it was observed that the common arrangement for fully-fixed connections in steel moment framed led to a brittle failure mode during earthquake events. For example, the Northridge earthquake of 1994 in Los Angles resulted in the brittle failure of fixed connections in steel moment frames in the zone where the beam flange was welded to the column face. This led to a weak, and un-ductile, performance of the connection and frame due to the formation of a plastic hinge in this critical area.

Following on from similar observations of brittle failures, different methods for strengthening fixed joints were proposed, including reinforcing the joint with externally bonded plates and effectively weakening the beam in line with the strong column/connection, weak beam principle. Researchers proposed a new type of joint, known as a reduced beam section (RBS) connection with the aim of moving the plastic hinge away from the column during seismic events thus delaying or preventing overall collapse. In RBS connections, the cross-sectional area of the beam is reduced at the beam ends by removing some of the top and bottom flanges (see Fig. 1(a), which is a schematic adapted from [1]). This reduces the plastic moment capacity in these regions and moves the critical section away from the column to the reduced beam section, thereby increasing the ductility of the connection.

Studies demonstrated that the amount of material reduction in the flanges as well as the distance between the reduced section to the column edge are influential to the ductility and strength of the frames [2]. Engelhardt et al. [3] demonstrated that reducing the flange width by more than 40-50% compared with the original cross-section could cause beam stability problems such as web buckling, torsional buckling, and local buckling in the compression flange. More studies have been conducted to understand the influence of floor slabs on the behaviour [4] as well as the effect of panel zone strength ratio on RBS connections [5]. Whilst RBS connections certainly improve the overall survivability of steel moment frames during an earthquake, they also have some disadvantages. They can lead to the beam being susceptible to lateral torsional buckling failure, which ultimately leads to extensive strength degradation in the

https://doi.org/10.1002/cepa.2320 wileyonlinelibrary.com/journal/cepa

joint. The reduced portion of the flange to support the web can result in local web buckling and also there can be some column twisting in deep column connections as a result of lateral torsional buckling of the beam.

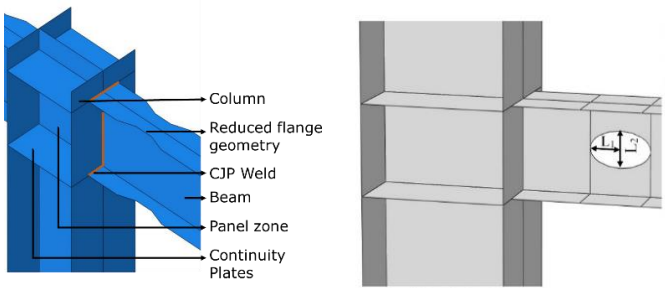

(a) (b)

Figure 1 Schematic view of (a) a typical RBS connection [1] and (b) a RWS connection

In this context, an alternative "beam weakening" strategy is to employ a reduced web section (RWS) connection, as shown in Fig. 1(b). In these, the web area is reduced by cutting an opening such as those found in cellular beams. RWS connections have been the subject of much fewer research studies compared with RBS connections, although more information been made available in recent years. Different opening arrangements have been examined including having two parallel slots on the beam web [6], rectangular openings [7] and circular openings [8]. It was shown that all reduce the stress concentrations in the connection, leading to ductile behaviour, and also result in greater distance between the location of the plastic hinge, in the beam, and the column edge. Design procedures have been proposed [9] in accordance with AISC 358 [10]. It was shown [11] that employing RWS connections rather than equivalent RBS arrangements significantly enhances the resistance to lateral-torsional buckling.

The current paper is concerned specifically with RWS moment connections under fire conditions. There is very little performance information available in the literature on this topic. Although the multi-hazard event of an earthquake, followed by a fire, is also relevant to this, the current paper is concerned with single-hazard fire events only. Fire is one of the key limit states for steel structures, owing to its high thermal conductivity, and typically high section factor (H_p/A where H_p is the perimeter of the section and A is the cross sectional area). Usually, steel structures are designed to have fire protection, which is very expensive, to insulate the key areas from unacceptable levels of structural degradation, when subjected to a standard fire. One of the key areas of a structure during an extreme event, like a fire, is the connections, which may be required to undergo large deflections without failure. For this reason, connections have been subjected to significant scrutiny from the research community in recent years (e.g. [12,13]). Studies such as these have led to the development of numerical and analytical models (e.g. [14,15]).

The current paper proceeds with a detailed description and analysis of a new fire test which was conducted at Tampere University in Finland in collaboration with Brunel University London and University College London. The principal aims of test were to (i) develop a fundamental understanding the fire behaviour of these details, and (ii) provide sufficient data so that a numerical model can be validated and then used to conduct a wider study. Accordingly, the important data recorded during the test is presented, including the deflections, fire resistance in minutes, failure mode and temperature profile and gradient at key locations.

2 Fire test

A fire test was designed and conducted on a reduced web section (RWS) connection to assess how this type of a connection behave under fire conditions.

2.1 Test specimen and set-up

The joint specimen consisted of two identical welded connections forming a double-sided beam-to-column joint configuration. Two horizontal IPE 140 steel sections were welded to the flanges of a vertical HEB 160 post with 6 mm fillet welds. In the joint region, the cross-section of the horizontal I-sections was reduced by creating elliptical web openings. The vertical steel section was reinforced with 8 mm thick web stiffeners and 10 mm thick web doublers in order to ensure that failure occurred in the reduced members. All of the I-sections and 10 mm steel plates were made from grade S355J2 carbon steel, in accordance with EN 10025-2:2019 [16], while the 8 mm plates were made using grade 355MC carbon steel, in accordance with EN 10149-2:2013 [17].

The testing furnace had a rectangular chamber with internal dimensions of 3000 mm × 3000 mm × 4000 mm (height × width × length). The specimen's vertical post was bolted to a steel loading frame located above the furnace, so the joint specimen hung from the frame; see Fig. 2(a) for a photographic image of the arrangement. An end plate of 400 mm × 300 mm × 20 mm (length × width × thickness) was welded to the end of the HEB 160 member, and the plate was fixed to the frame above the furnace with four bolts. The joint was loaded using two hydraulic loading jacks fixed to the loading frame, as shown in Fig. 2(b). Two long 1470 mm × 220 mm × 10 mm (length × width × thickness) steel plates were welded to the ends of the horizontal members. These plates were bolted to the loading jacks above the furnace roof. To limit their thermal elongation, these plates were fire protected. The specimens' boundary conditions can be treated as rigid supports; the ends of the horizontal members were restricted from rotating but could move upwards.

(a) (b)

Figure 2 Test furnace arrangements including (a) a photographic image of the specimen inside the furnace before testing and (b) the loading jacks outside of the furnace

2.2 Instrumentation

The joint specimen was heavily instrumented during the

test, with thermocouples and linear variable differential transducers (LVDTs) to measure temperatures, displacements and deformations. The data from these devices was essential for the later validation of the numerical model. The steel temperatures were measured using 31 thermocouples installed in pre-drilled holes in the steel sections. The displacements of the horizontal beam stub ends were measured and monitored by the jacks located outside the furnace. In addition, joint deformations were measured using wires and steel screws fixed to the top flange of the IPE sections in 6 different locations. A molybdenum wire was attached to a steel screw, and pulled through two fixed pulleys outside the furnace and connected to an LVDT. The pulleys changed the direction of the molybdenum wire, and a 1 kg weight tied at the end kept the wire straight during the experiment. The elongation of the wire during heating was considered and eliminated from the measured displacements using a reference wire.

2.3 Tensile coupon tests

Tensile coupon tests were carried out in order to determine the mechanical properties at ambient temperature. The test pieces were prepared from the same batch of steel members as the tested joints and tested, as shown in Fig. 3, and the tests were conducted in accordance with SFS EN 10002-1:2002 [18]. Three test pieces were flame-cut from the beam flange and web in the longitudinal direction of the IPE and HEB sections. Three pieces were also cut from the 8 mm and 12 mm thick steel plates, used in the joint configuration. The strains were calculated from the extension measurements using an extensometer over a gauge length of 50 mm. The average values for each of the measured steel material properties, are listed in Table 1, where E, f_y and f_u are the Youngs modulus, yield strength and ultimate tensile strength, respectively, and ε_u is the ultimate strain.

Table 1 Mechanical properties of the steel components

Profile		ε_u %	f_y N/mm²	E kN/mm²	f_u N/mm²
IPE 140	Web	24.3	458	208	538
	Flange	23.6	401	206	540
HEB 160	Web	20.8	462	207	555
	Flange	23.8	446	206	538
10 mm plate		22.4	553	203	584
8 mm plate		19.1	467	227	546

Figure 3 Steel sections and plates from which the test coupons were cut for material testing.

2.4 Test procedure

The experimental tests were divided into two phases. In the first phase, the specimens were loaded with the target axial force until the joint was stable. In the second phase, the specimens were exposed to an ISO-834 standard fire curve until failure, then allowed to cool. Two identical tensile forces were applied to the IPE beam stub members through loading jacks and the long steel plates welded to the stubs. These forces resulted in a shear force and bending moment acting on the beam-to-column joints. The loading was kept constant throughout the test. The level of loading represents approximately 25% of the static design moment resistance of the joint at ambient temperature. The resistance was calculated according to EN 1993-1-8 [19] using the steel material properties determined in tensile coupon tests described previously. The estimated joint bending moment resistance was 24 kNm and the corresponding applied jack loading was 20 kN per jack.

3 Test results

The test was terminated and the burners were switched off 16.5 minutes after the commencement of the test as the displacements began to increase significantly and very quickly. The end displacements of the IPE beam stub members (as measured by LVDTs 7 and 8) and the local joint displacements at the end of the web opening (LVDTs 1 and 6) are presented in Fig. 4. The four curves show very similar shape. Based on the joint displacement curves, the rate of deflections at the web opening began to increase rapidly at 15 minutes indicating that the joint was beginning to fail. The measured displacements of the other LVDTs (2-5) were insignificant. The furnace temperature and the temperatures of the IPE members in the vicinity of the web opening are presented in Fig. 5. The results show that the temperature distribution of the IPE cross-section was uniform. After 15 minutes of heating, when the specimen began to fail, the web and flange temperatures at the opening were 703 ℃ and 692 ℃, respectively. The failure mode observed in the test was a Vierendeel mechanism at the opening, as shown in Fig. 6.

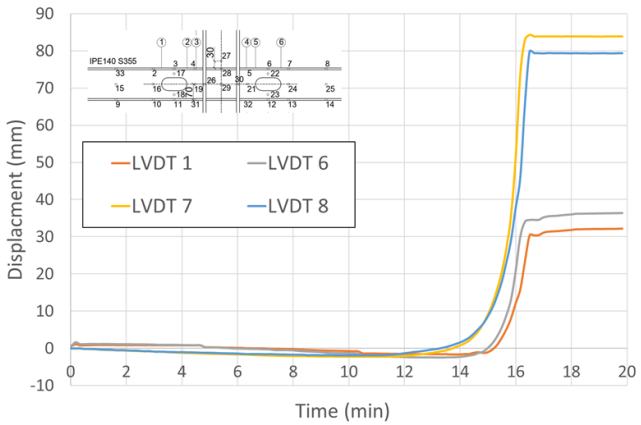

Figure 4 Development of displacement at different locations in the beam versus time

Figs. 8-10 present a more detailed view of the change in temperature, with time, at various key locations in the beams, column and beam-to-column interface, with time. Firstly, Fig. 7 presents the variation in temperature measured by the thermocouples located along the top flanges

of the beam members. It is clear that the temperatures did not rise quite as rapidly for the thermocouples located near the column face, as some protection was offered in this location.

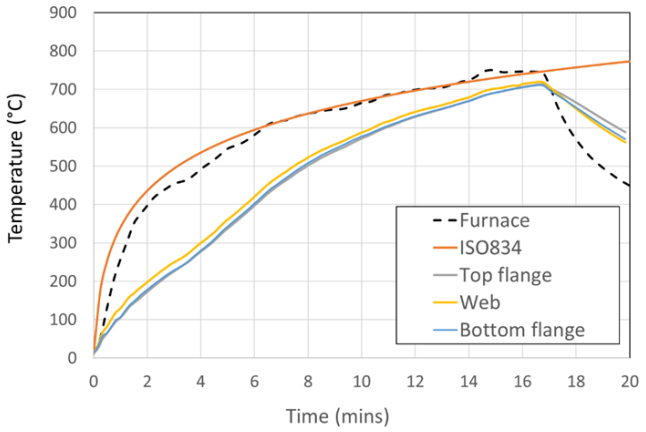

Figure 5 Measured furnace and steel beam temperatures at the vicinity of the web opening

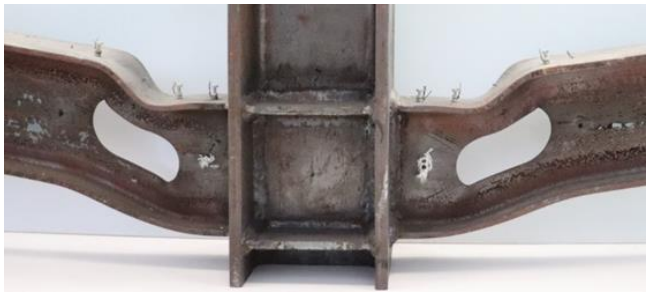

Figure 6 Deformed RWS connection after the fire test

A similar phenomenon is also visible in Fig. 8 which presents corresponding data at locations in the web near the opening; the results from the thermocouples in the bottom flange are not presented here for brevity but are similar. As before, the thermocouples closest to the column face measured the lowest temperatures and also took longer to increase in temperature, compared with the other web/flange locations.

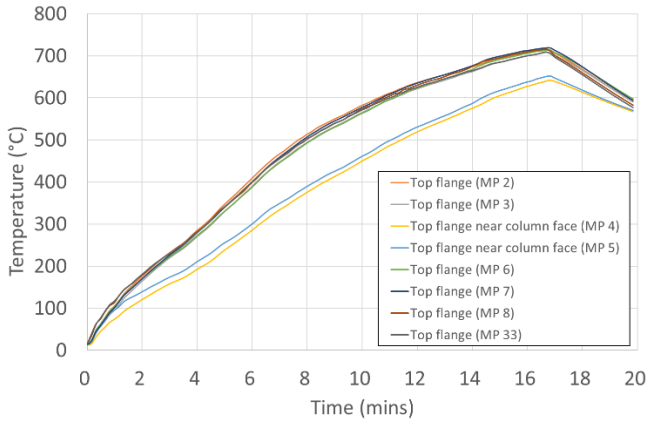

Figure 7 Temperature versus time at various locations along the beams top flanges

Interestingly though, through comparison between all of the data presented in Figs 7 and 8, it is observed that the peak temperatures of just over 700°C were similar in value at the web and top flanges and were also measured in all locations, at almost identical times (around 16.5 minutes after the test began); this was also observed in the bottom flanges. This indicates that all locations in the steel beam are vulnerable to rapid elevated temperature spread through the section.

Fig. 9 presents the elevated temperature versus time data at locations at the beam to column interface, including the various stiffener and doubler plates as required for seismic design. In this case, the web doubler plate was the slowest to reach each level of elevated temperature, most likely owing to its orientation relative to the application of temperature.

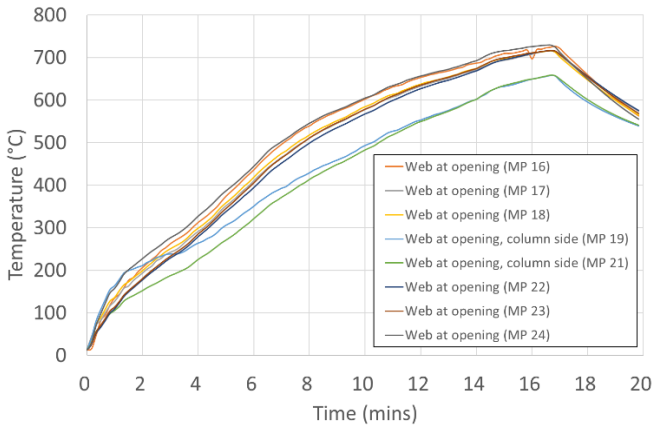

Figure 8 Temperature versus time at various locations in the web, near the opening

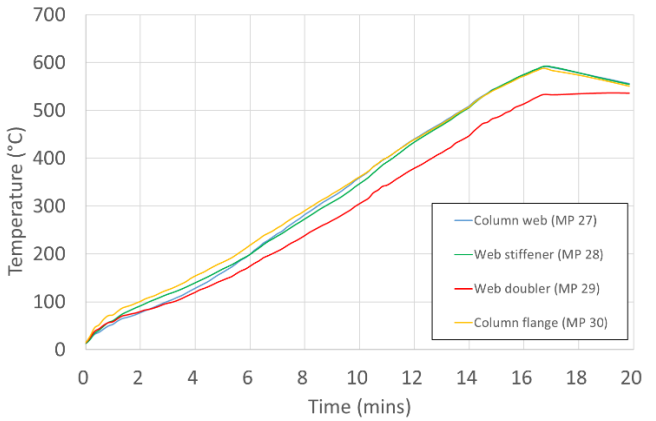

Figure 9 Temperature *versus* time at various locations in the beam/column region

4 Numerical analysis

A finite element numerical model was developed in order to further understand the key behavioural aspects of RWS connections in fire; a brief overview is presented herein owing to page limits. The model was developed in the Abaqus software [20] and then validated using the test results previously described. The numerical model was capable of capturing both the geometrically and materially nonlinear behaviour of reduced web section connections in fire conditions.

4.1 General details

The RWS connection was modelled using shell elements called S4RT which are available in the Abaqus library. The

S4RT shell element was used to define both the beam and column components. This is a 4-noded, thermally-coupled, doubly-curved element, with reduced integration and finite membrane strains. It has four corner nodes, each with six degrees of freedom, and is suitable for either thick or thin shell applications. The model was first developed based on the test details as previously described, as the results are employed for validation of the approach.

A mesh sensitivity study was performed to identify an appropriate mesh density to achieve suitably accurate results whilst maintaining computational efficiency. Following this, a mesh size of 15 mm for the region near the connection and 20 mm for the other areas was employed. The analysis was run as a mechanical-thermal analysis. Accordingly, first, an initial mechanical load was applied and then the elevated temperature was applied, based on the time-temperature response during the testing program.

4.2 Material properties

The ambient temperature material properties, as given in Table 1, were employed to represent the steel stress-strain response in the model. At elevated temperature, the reduction factors as given in Eurocode 3 Part 1-2 [21] were employed to represent how each of the key mechanical characteristics such as 0.2% proof strength, ultimate strength, ultimate strain and the elastic modulus, vary at different levels of elevated temperature. The model also adopted the coefficient of thermal expansion, the specific heat and the thermal conductivity for carbon steel based on the guidance given in Eurocode 3 Part 1-2 [21]. According to Eurocode 3 Part 1-2, the surface emissivity for steel is considered to be 0.4, and the convective heat transfer coefficient of 25 W/m^{2}K; these values were employed in the FE analysis [22].

4.3 Boundary and loading conditions

The boundary and loading conditions of the connection were modelled to simulate the exact conditions of the test specimen discussed previously this paper. The experimental test was divided into two phases. In the first phase, the specimen was loaded with the target axial force and this was maintained at a constant value until the joint was stable. Then, in the second phase, the specimens were exposed to an ISO-834 standard fire until failure occurred. Following this, the load was removed from the test specimen and it was allowed to cool naturally in the furnace.

Two identical concentrated forces equal to 20 kN each were applied to the IPE 140 355 beam members through loading jacks and the long steel plates welded to the stubs. The self-weight of the elements was taken into account in the simulation. Then, the heat was applied and a coupled temperature-displacement analysis was performed. For the boundary conditions, the displacement at the top of the column was restrained in all directions.

4.4 Comparison with the test results

Fig. 10 presents the deflection *versus* temperature response obtained during the physical experiment together with the corresponding values predicted by the finite element model. The results are compared for the joint displacements at the end of the web opening (represented by LVDT 6 in the test) and also for the end displacements of the beam members (as measured by LVDT 7). It is clear from the data presented that the FE model provides a realistic response compared with the experimental values. The response can be generally divided into two phases. First, up to a temperature of around 680°C, there was very low levels of deflection in the arrangement owing to the absence of any horizontal resistance to the development of thermal expansion. Then, once the temperature increased beyond 700°C, the behaviour of the connection entered the second phase and the deflections suddenly increased significantly. At this temperature, there was a significant reduction in both the strength and stiffness of the steel material. The concentration of stress at the corners of the web openings lead to buckling in the flanges directly above the opening, leading to failure. These phenomena, which were observed in the test data, were very well replicated by the FE model.

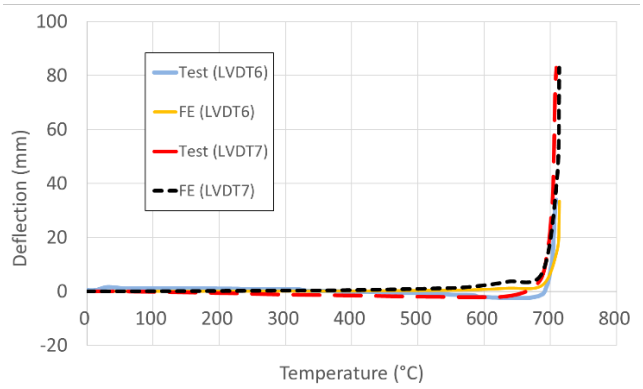

Figure 10 Deflection versus temperature of experimental and numerical models for the RWS connection at the web opening (LVDT6) and beam end (LVDT7)

In addition, the Von Mises stress distribution and deformations obtained from the finite element model were compared with the corresponding behaviour during the experiment. As shown in Fig. 11, the locations of the maximum Von Mises stresses in the finite element simulation, represented by the red/orange colours in the figure, correspond well with the location of significant deformations in the experimental specimens (Fig. 6). Moreover, the overall deflected shape is accurately depicted, in particular in the region of the web openings. Overall, from the comparisons presented between the experimental and numerical results, it is concluded that the finite element model is capable of providing an accurate depiction of the RWS behaviour in fire.

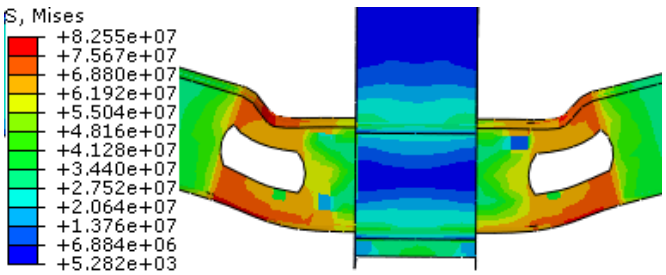

Figure 11 Deflected specimen from the numerical model illustrating the Von Mises stress distribution

5 Comparison study

The validated finite element model was employed to conduct an investigation into the behaviour of RWS connection in fire and to assess the behaviour in comparison to other three other joint configurations. These include a full beam section (FBS), a reduced beam section (RBS) with radial cuts in the flange on both sides of the web and the reduced web section (RWS) joint arrangements. All of the connections were modelled using the S4RT shell elements as previously described. For the RBS connection, the cut taken from the flanges is at an identical location to the web opening in the previous analysis, beginning 70 mm from the column face. The total area of steel removed was the same for the RWS and RBS connections.

In this study, the material properties of the steel components were identical to those employed previously and as described in Table 1, together with the reduction factors given in Eurocode 3 Part 1-2 [21]. Fig. 12 presents the temperature *versus* deflection response for each of the three connection types, under identical loading and fire conditions. It is observed that the performance of the RWS and FBS joints were similar, but the RBS joint experienced runaway failure at a lower temperature. However, the arrangements failed by different modes, as indicated by the deformed shapes presented in Fig. 13. The RBS arrangement clearly fails by lateral torsional buckling due to the cutting of the flange. On the other hand, it is also shown that the stresses at the column face in the RWS connection are reduced compared with in the beam section where the web openings exist. Therefore, this connection is successful at achieving the "strong column-weak beam" principle, even during the fire event.

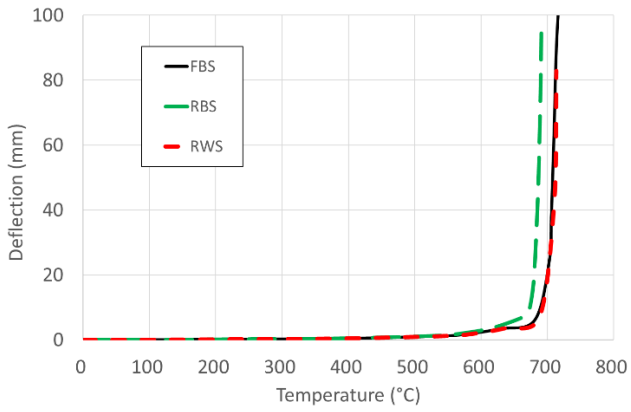

Figure 12 Temperature-deformation curve of the FBS, RBS and RWS connections

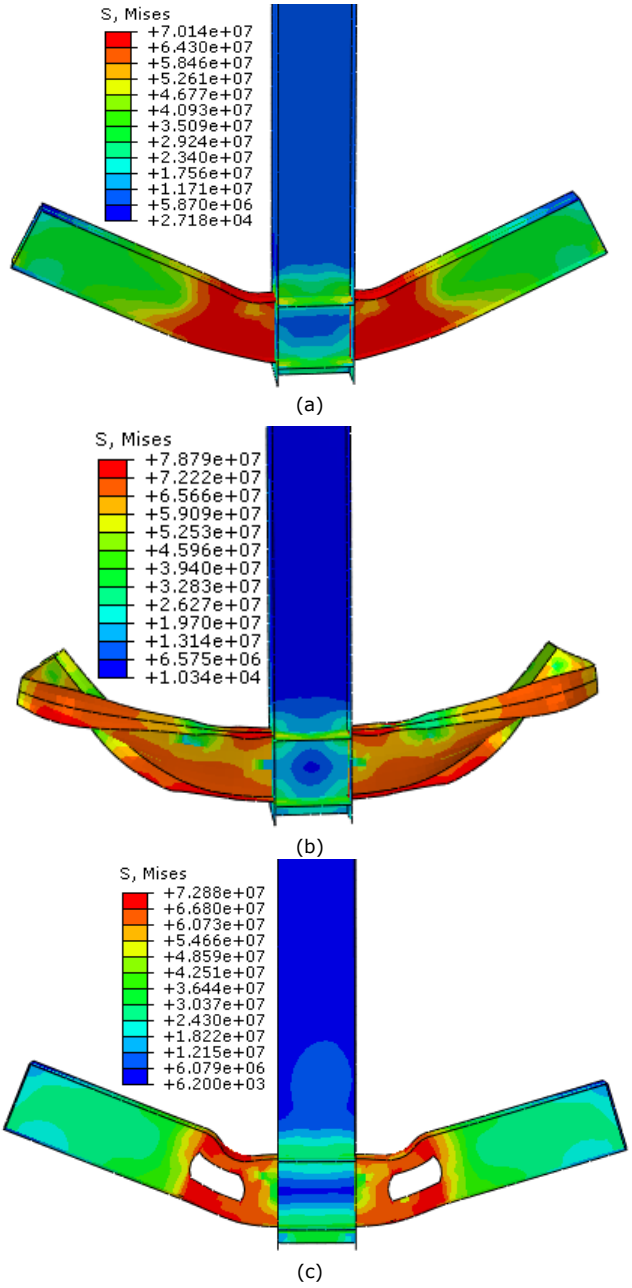

Figure 13 Images of the deflected specimen with Von Mises stress distributions for (a) FBS, (b) RBS and (c) RWS joint arrangement

6 Conclusions

This paper presents a detailed description of a fire test conducted on an RWS connection. These arrangements are typically specified in steel framed structures designed for seismic events, in line with the strong column-weak beam principle. The test showed that the arrangement performed well in fire, with failure occurring in the beam rather than the column, as desired. A brief overview of finite element model is also presented, and the results from this initial analysis suggests that the RWS connection performs as well as a fully fixed connection, and a RBS connection, in terms of survival time, but has a more favourable failure mode.

7 References

[1] Naimi, S., Celikag, M., & Hedayat, A. A. (2013) *Ductility enhancement of Post-Northridge connections by multilongitudinal voids in the beam web*. The Scientific

World Journal, 2013, 1–14. https://doi.org/10.1155/2013/515936.

[2] Shen, J., Kitjasateanphun, T., & Srivanich, W. (2000) *Seismic performance of steel moment frames with reduced beam sections*. Engineering Structures, 22(8), 968–983. https://doi.org/10.1016/s0141-0296(99)00048-6.

[3] Engelhardt, Michael D., Winneberger, Ted, Zekany, Andrew J., Potyraj, Timothy J. (1998) *Experimental Investigation of Dogbone Moment Connections*. Engineering Journal, American Institute of Steel Construction, Vol. 35, pp. 128-139.

[4] Jones, S. L., Fry, G. T., & Engelhardt, M. D. (2002) *Experimental evaluation of cyclically loaded reduced beam section moment connections*. Journal of Structural Engineering, 128(4), 441–451. https://doi.org/10.1061/(asce)0733-9445(2002)128:4(441).

[5] Soliman, A. A., Ibrahim, O. A., & Ibrahim, A. M. (2018) *Effect of panel zone strength ratio on reduced beam section steel moment frame connections*. Alexandria Engineering Journal, 57(4), 3523–3533. https://doi.org/10.1016/j.aej.2018.07.017.

[6] Swati, A. K., & Gaurang, V. (2014) *Study of steel moment connection with and without reduced beam section*. Case Studies in Structural Engineering, 1, 26–31. https://doi.org/10.1016/j.csse.2014.04.001.

[7] Hedayat, A. A., & Celikag, M. (2009) *Post-northridge connection with modified beam end configuration to enhance strength and ductility*. Journal of Constructional Steel Research, 65(7), 1413–1430. https://doi.org/10.1016/j.jcsr.2009.03.007.

[8] Davarpanah, M., Ronagh, H., Memarzadeh, P., Behnamfar, F. (2020) *Cyclic behaviour of elliptical-shaped reduced web section connection*. Structures, 24, 955–973. https://doi.org/10.1016/j.istruc.2020.02.016.

[9] Boushehri, K., Tsavdaridis, K. D., & Cai, G. (2019) *Seismic behaviour of RWS moment connections to deep columns with European sections*. Journal of Constructional Steel Research, 161, 416–435. https://doi.org/10.1016/j.jcsr.2019.07.009.

[10] Seismic provisions for Structural Steel Buildings, ANSI/AISC 341-10. (2011) *Structural Analysis and Design of Tall Buildings.* 355–410. https://doi.org/10.1201/b11248-8.

[11] Davarpanah, M., Ronagh, H., Memarzadeh, P., & Behnamfar, F. (2020) *Cyclic behaviour of elliptical-shaped reduced web section connection*. Structures, 24,955–973. https://doi.org/10.1016/j.istruc.2020.02.016.

[12] Dai X. H., Wang Y.C., Bailey C.G. (2009) *An experimental study of structural behaviour of joints in restrained steel frames in fires*. International conference, Application of Structural Fire Design, pp. 19–20, February 2009.

[13] Tsavdaridis, K. D., & Papadopoulos, T. (2016) *A Fe parametric study of RWS beam-to-column bolted connections with cellular beams*. Journal of Constructional Steel Research, 116, 92–113. https://doi.org/10.1016/j.jcsr.2015.08.046.

[14] Davarpanah, M., Ronagh, H., Memarzadeh, P., Behnamfar, F. (2020) *Cyclic behavior of welded elliptical-shaped RWS moment frame*. Journal of Constructional Steel Research, 175, 106319. https://doi.org/10.1016/j.jcsr.2020.106319.

[15] Hedayat, A. A., & Celikag, M. (2009) Post-northridge connection with modified beam end configuration to enhance strength and ductility. Journal of Constructional Steel Research, 65(7), 1413–1430. https://doi.org/10.1016/j.jcsr.2009.03.007.

[16] *EN 10025-2 Hot rolled products of structural steels, Part 2: Technical delivery conditions for non-alloy structural steel* (2019) European Committee for Standardization (CEN). https://doi.org/10.3403/03152996.

[17] *EN 10149-2 Hot rolled flat products made of high yield strength steels for cold forming, Part 2: Technical delivery conditions for thermomechanically rolled steels* (2013) European Committee for Standardization (CEN). https://doi.org/10.3403/30239495.

[18] *SFS EN 10002-1 Metallic materials. tensile testing, Part 1: Method of test at ambient temperature* (2002) European Committee for Standardization (CEN). https://doi.org/10.3403/30144369.

[19] *EN 1993-1-1-8 Eurocode 3: Design of Steel Structures, Part 1-8: Design of Joints* (2005) European Committee for Standardization (CEN). https://doi.org/10.1680/dgte3.31630.

[20] *Abaqus/CAE User's Guide* (2017) Dassault Systems. http://130.149.89.49:2080/v6.14/index.html.

[21] *EN 1993-1-1-2 Eurocode 3: Design of Steel Structures, Part 1-2: Design of Joints* (2005) European Committee for Standardization (CEN). https://doi.org/10.1680/dgte3.31630.

[22] *EN 1991-1-1-2 Eurocode 1: actions on structures. Part 1-2: General actions, Actions on structures exposed to fire* (2002) European Committee for Standardization. https://doi.org/10.3403/02700262.